Targeting Uropathogenic *Escherichia coli*, a Virulent Strain of Urinary Tract Infection: In Silico Study of *Aloe barbadensis miller* Phytoconstituents

Abstract

The most frequent pathogen linked to the development of UTIs is Uropathogenic *Escherichia coli* (UPEC). Thus, inhibiting the UPEC protein target (PDB ID 8BVD) would be a viable treatment approach. This study used molecular docking and dynamics to investigate *Aloe barbadensis miller* antibacterial activity against UPEC bacteria. The Phytoconstituents of *Aloe barbadensis miller* such as aloe-emodin, cholic acid, and flavonol were downloaded from the PubChem database with nitrofurantoin as a control drug and investigated against the target molecule. Some potential parameters such as docking scores, absorption, distribution, metabolism, excretion, toxicity (ADMET), oral bioavailability, root mean square deviation (RMSD), root mean square fluctuation (RMSF), hydrogen bonding, radius of gyration, and total energy of the system were examined. According to the docking score results, all ligands showed excellent candidacy as an inhibitor of the 8BVD molecule. The score order was aloe-emodin (-6.6 kcal/mol), cholic acid (-6.8 kcal/mol), flavonol (-6.8 kcal/mol) and nitrofurantoin (-6.1 kcal/mol). Every ligand seemed to possess favorable drug-likeness characteristics and oral bioavailability. Molecular dynamics investigation showed that every ligand demonstrated a strong candidate for an inhibitor in its vicinity of 20 ns. Contrary to cholic acid, which appears to be more stable, aloe-emodin and flavonol showed comparatively high fluctuations. The results of this study imply that the chosen Phytoconstituents may be employed as 8BVD protein inhibitors to combat urinary tract infections. Nevertheless, the room is still available for more research to validate the particular mechanism of UTI treatment through clinical and experimental methods.

Key words: Molecular docking, Molecular dynamics, Phytoconstituents, Uropathogenic Escherichia Coli, Virulent Strain.

Introduction

Urinary tract infection (UTI) is the most prevalent infectious disease identified worldwide, particularly in many developing countries (Mwang'onde & Mchami 2022). It is one of the predominant microbial disorders in clinical practice. Approximately 150 million people are believed to have UTIs globally with significant morbidity and high medical costs per annum (Zagaglia et al., 2022). The annual societal costs of these infections in the USA alone are estimated to be around US dollar 3.5 billion, including medical expenses and lost productivity (Flores-Mireles et al., 2015). Most of the population visiting healthcare facilities, especially those in developing and middle-income countries, perceived the disease more often. This includes schoolchildren, students in higher learning institutions, and any member of the public, mostly women living in communal camps or organizations. There are two clinical classifications for UTIs; complicated and non-complicated types. Several factors that impair the urinary tract or host defense have been connected to complicated UTIs including immunosuppression, renal failure, pregnancy, urinary blockage, urine retention, and indwelling catheters or other drainage, while

non-complicated UTIs were associated with the health of patients showing the absence of structural or neurological urinary tract abnormalities (Flores-Mireles et al., 2015 &Zagaglia et al., 2022).

Uropathogenic E. coli (UPEC) is a major cause of UTIs leading to a significant burden on public health (Mousavifar et al., 2023). UPEC are the most commonly isolated bacteria globally accounting for 80 to 90%, compared to other gram-negative and gram-positive bacteria (Terlizzi et al., 2017, Seifu & Gebissa 2018, Mwang'onde & Mchami 2022). The bacteria have stains that change from their commensal state as intestinal flora develop and remain in the urinary tract, and exhibit a wide range of virulence factors and tactics, allowing them to infect and cause illnesses in the urinary tract (Shah et al., 2019).

Antibiotics such as nitrofurantoin, β-lactams, trimethoprim, and quinolones have been used as routine treatments of UTIs in many developing countries. Although some of these medications have been shown to be effective in reducing the clinical symptoms of UTIs, recurring and chronic infections still affect many individuals (Asadi Karam et al., 2019). Phytochemicals derived from natural products have been used in drug development, and these products have been considered in the chase for the novel medication combined with other strategies like computational method (Yuan et al., 2016).

Computational methods of molecular docking and dynamics are effective for identifying new drugs and are thus widely used in the pharmaceutical industry (Fatriansyah et al., 2022). Computer-aided drug discovery and design may shorten the time taken for a medicine to reach the consumer market, in addition to lowering the expenses involved in drug discovery by guaranteeing that the best lead molecule can enter animal trials (Preman et al., 2022).

Medical plants with antibacterial and anti-inflammatory qualities have been used recently to treat a wide range of infectious diseases in humans. Aloe vera (*Aloe barbadensis miller*) is a well-known therapeutic plant used against UPEC (Goudarzi et al., 2018). Its phytoconstituents have major pharmacological features and are widely recognized for their numerous health benefits including its ability to boost immunity, reduce inflammation, prevent sunburn, age prematurely, and anti-cancer. (Maan et al., 2018). As a result, they are becoming increasingly popular among clinical researchers as a way to provide cost- and time-efficient therapeutic options for eradicating UTIs (Goudarzi et al., 2018 & Newman and Cragg 2020).

Therefore, this study used computational methods to ascertain the antibacterial properties of aloe-emodin, cholic acid, and flavonol derived from *Aloe barbadensis miller* and nitrofurantoin as control drugs. Molecular docking and dynamic studies were conducted to evaluate important parameters such as docking score, hydrogen bond, root mean square deviation (RMSD), root mean square fluctuation (RMSF) radius of gyration, and total energies of the system.

Materials and Methods

Materials Collection

The structures of aloe-emodin, cholic acid, flavonol, and nitrofurantoin were downloaded from the PubChem library as 3D conformers and saved as a structure data file (sdf) (Kim et al., 2023). Their molecular structures are shown in (Figure 1).

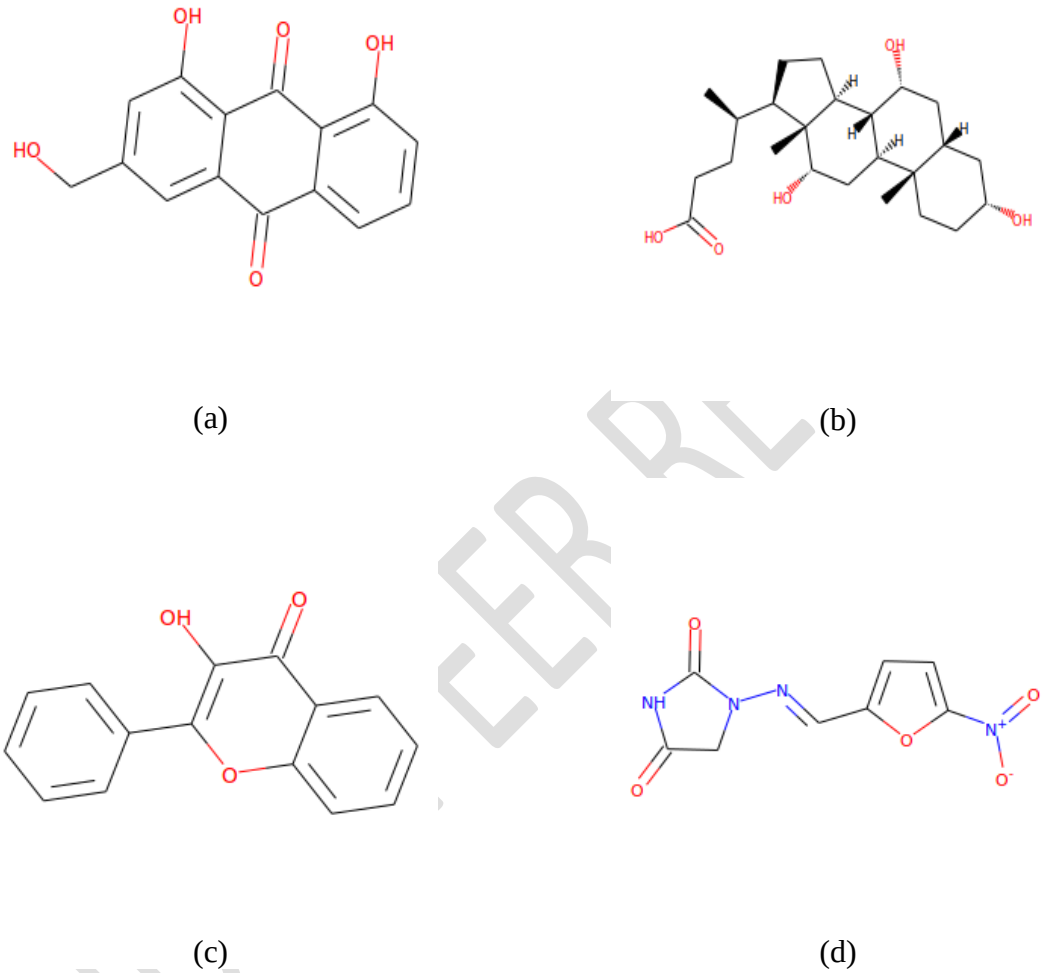

Figure 1. Molecular structures of the compounds (a) aloe-emodin, (b) cholic acid, (c) flavonol and (d) nitrofurantoin

Protein Selection and Preparation

The protein molecule UPEC type 1 fimbrial (FimH) lectin domain in complex with mannose C-linked to quinolone was downloaded from Protein Data Bank (PDB ID: 8BVD) (Mousavifar et al., 2023). Using the X-ray diffraction method the desired macromolecule was obtained with a resolution of 3.00 Å an R-value free of 0.303 and an R-value work of 0.251, indicating good quality and high resolution of the molecule (Kleywegt & Jones, 1997). UPEC type 1 FimH complex molecules are desirable substitutes for antibiotic therapy and prophylactic measures against acute or urinary tract infections (Abe et al., 2008 & Mousavifar et al., 2023). Protein receptors were prepared using the Usf Chimera software by removing solvent and ligand molecules from the 8BVD target, removing residues selenomethionines to methionine's, adding hydrogen atoms, and

charging the protein for protein optimizations. (Gurisha et al., 2024). For site-specific docking, the ligand coordinates for the center at X: 26, Y: 58, Z: -9, and box with dimensions of X: 13, Y: 7, and Z: 10 were designed. The ready-to-dock protein receptor was saved in the mol2 file.

Ligand Preparations

The Phytoconstituents of *aloe barbadensis miller* were recovered from the commercial PubChem library that was easily accessible. The ligands were prepared using Ucsf Chimera software, which optimized them to match the protein and saved the results as mol2 in the working directory (Pettersen et al., 2004).

Molecular Docking

Docking is a computational technique that forecasts the interaction between small molecules (ligands) and proteins (enzymes). The program's score function analyzes the docking results; a lower value indicates a better interaction (Stanzione et al., 2021). Molecular docking was performed using Ucsf chimera software that can be expanded upon to facilitate the interactive conception and investigation of molecular structures and associated data. This includes sequence alignments, density maps, conformational ensembles, docking results, trajectories, and supramolecular assemblies (Pettersen et al., 2004).

The protein receptor and the minimized ligand saved in the mol 2 file were selected and opened in the auto dock vina window. The receptor and ligand were selected as outputs, and the coordinates for the center and the size for site-specific docking were generated in the boxes. The executable location path for the vina and vina splits was set and docking was performed.

Physicochemical, Pharmacokinetics, Drug-Likeness and ADMET Prediction

The pharmacokinetic and pharmacodynamic profiles of a drug are largely determined by its physicochemical qualities, which are crucial for boosting a drug candidate’s chances of success during the preclinical development process (Camp et al., 2015). Drug candidates fail in clinical trials for a variety of reasons, but the two main reasons are undesirable pharmacokinetic characteristics and unacceptable toxicity (Honorio et al., 2013). Drug candidates must thus be chosen carefully by researchers to ensure that effectiveness, absorption, distribution, metabolism, excretion, and toxicity are all balanced (Yang et al., 2019). On the other hand, certainly, the inhibition of these isoenzymes (CYP1A2, CYP2C19, CYP2C9, CYP1A2, CYP2D6, and CYP3A4) contributes to pharmacokinetics. Related drug-drug interactions can result in toxic or other unfavorable side effects because of the reduced clearance and buildup of the drug or its metabolites. In this study, the three best-scoring ligands were evaluated: physicochemical, pharmacokinetic (PK), Drug-Likeness and ADMET Prediction using pkCSM and SwissADME web tools (Pires et al., 2015 & Daina et al., 2017).

Bioavailability Radar

Drug likenesses are quickly assessed by using bioavailability radar, in this case, six physiochemical parameters like lipophilicity, size, polarity, solubility, flexibility, and saturation

were considered (Udugade et al., 2019). SwissADME software was used to conduct thorough and accurate testing (Diana et al., 2017).

Molecular Dynamics

The GROMACS software was used to perform molecular dynamics simulations on 8BVD-CID10207, 8BVD-CID221493, 8BVD-CID11349, and 8BVD-CID6604200 at 300 K with a CHARMM27 force field, and the hybrid ligand structure and force field properties of the chosen ligand were determined using Swiss Param (Van Der Spoel et al., 2005).

Free 8BVD, 8BVD-CID10207, 8BVD-CID221493, 8BVD-CID11349, and 8BVD-CID6604200 were solvated with water in a cubic box with a basic diameter of 1 nm with all default settings. Using constant volume and periodic boundary conditions, the system temperature was raised from 0 to 300 K throughout the equilibration time (1000 ps). The system was then lowered using the 1000 sharpest decline steps. The created trajectories were utilized to evaluate each complex's behavior as well as the system's overall stability. Calculations of the hydrogen bond, root mean square deviation, root mean square fluctuation, radius of gyration, and total energies were used to examine the variations in the macromolecule and macromolecule-ligand complex system (Salaria et al., 2022).

The equilibration process was divided into two phases using the number of particles, system volume and temperature (NVT) ensemble, and number of particles system pressure and temperature (NPT) ensemble. The C backbone atoms of the original structures were confirmed, while all the other atoms were free to move in both NVT and NPT. Molecular dynamics (MD) was then run at 300k with a 20ns time frame. The GROMACS analysis modules were used to examine the trajectories obtained. UCF Chimera and Maestro were used to visualize MD movies and interaction diagrams, respectively (Walters et al., 2014).

Results and Discussion

Docking Scores

Molecular docking scores for aloe-emodin, cholic acid, flavonol, and nitrofurantoin are shown in Table 1. According to the scores, the ligand cholic acid has the lowest affinity for binding to the 8BVD target. A lower docking score indicates that ligand and target binding are more stable. The different structures bound to the target caused variations in ligand-target interactions which led to different docking scores (Fatriansyah et al., 2022) (Figure 2). Small molecules of cholic acid have been reported as potential lead drugs for the treatment of bacterial infections (Wu et al., 2023).

Table 1. Docking score for ligand-protein target

PubChem ID	Molecular Formula	Name	Docking Scores (kcal/mol)
10207	$C_{15}H_{10}O_5$	Aloe-emodin	-6.6
221493	$C_{24}H_{40}O_5$	Cholic Acid	-6.8
11349	$C_{15}H_{10}O_3$	Flavonol	-6.7
6604200	$C_8H_6N_4O_5$	Nitrofurantoin	-6.1

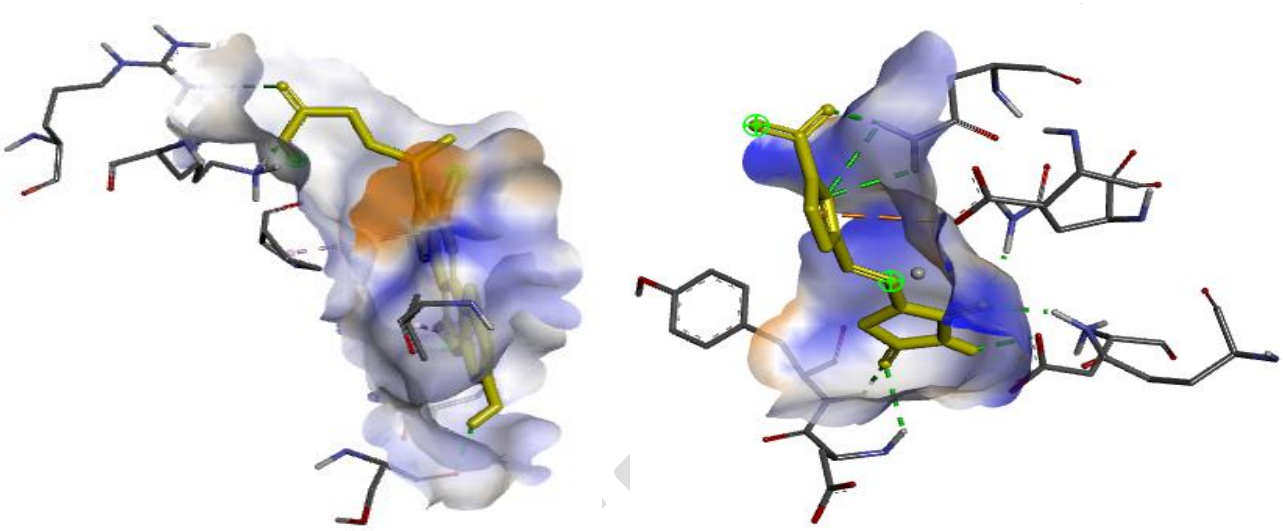

(a) (b)

Figure 2. Visualization of hydrophobic interaction between 8BVD with cholic acid ligand (a) and (b) nitrofurantoin

Physicochemical, Pharmacokinetics, Drug-Likeness and ADMET Prediction

A molecule needs to have the ideal pharmacokinetics and safety profile in addition to the intended biological functions to be taken into consideration as a potential therapeutic candidate (Hu et al., 2018). One of the biggest challenges for oral medicine is its ability to cross the intestinal epithelial barrier, which affects the rate and degree of human absorption (Rao et al., 2020). The selected compounds have an intestinal absorption rate of more than 60%, which is extremely high (Table 2). The selected molecules are non-hepatotoxic, do not cause skin sensitization, are non-permeable to the central nervous system (CNS) and blood-brain barrier (BBB), and exhibit negative AMES toxicity. It can also be reported that all ligands in this assessment permeate colon carcinoma cell 2 (CaCo-2) although aloe-emodin seems to have a low penetration potential.

The metabolic enzyme cytochrome P450 (CYP450) was examined and tested in the context of metabolism. The results indicating that, aloe-emodin and flavonol are potential inhibitors of CYP1A2, CYP1A2, and CYP3A4. Every ligand was also examined for toxic risks, such as hepatotoxicity, and the findings demonstrated that none of the substances could harm or impair the liver (Figure 2). The combination of the drug-likeness and ADMET properties suggested that aloe-emodin, flavonol, and cholic acid could be good options to inhibit the target in UTI drug development. According to the available data, aloe-emodin has a wide range of pharmacological effects such as anti-inflammatory, antibacterial, neuroprotective, hepatoprotective, and anti-tumor

effects (Dong et al., 2020). Cholic acid has been described to exhibit antibacterial, anti-viral, anti-fungal, anti-malaria, anti-tubercular, anti-tumor, and anti-allergic. It is a useful building block that can be used to create new molecules and a variety of compounds (Kishua & Siva, 2010).
Flavonol is a ketone group of flavonoid (Panche et al., 2016). They are considered antioxidant, anti-mutagenic, anti-inflammatory, and anti-carcinogenic. In addition to these abilities, they also alter the activities of important cellular enzymes (Burak & Imen, 1999).

Table 2: ADMET prediction of the highest scoring Phytoconstituents

Properties	**Model name**	**Predicted Value**				
		CID 10207	**CID 221493**	**CID 11349**	**CID 6604200**	**Unit**
Absorption	Water solubility	-3.104	-3.763	-3.683	-2.906	mol/L
	P-gp substrate	No	Yes	No	No	-
	P-glycoprotein	No	Yes	No	No	-
	Gastrointestinal absorption	High	High	High	High	-
	Caco-2 permeability	-0.233	0.597	1.263	-0.013	cm/s
	Intestinal absorption(%	74.179	61.546	94.776	79.533	-
Distribution	BBB permeability	-0.729	-0.716	0.462	-0.9	Log BB
	VDss (human)	0.671	-0.804	0.214	-0.544	Log L/kg
	Fraction unbound	0.226	0.171	0.151	0.54	Fu
	CNS permeability	-0.2466	-2.344	-1.733	-3.18	Log Ps
	Leadlikeness	Yes	No	No	No	-
Metabolism	Inhibitor CYP1A2	Yes	No	Yes	No	-
	CYP2C19	No	No	Yes	No	-
	CYP2C9	No	No	No	No	-
	CYP2D6	No	No	Yes	No	-
	CYP3A4	Yes	No	Yes	No	-
	CYP1A2	Yes	No	Yes	No	-
Excretion	Total Clearance	0.008	0.653	0.233	0.665	ml/min/kg
	Renal OCT2 substrate	No	No	No	No	-
Toxicity	Skin sensitization	No	No	No	No	-
	Hepatotoxicity	No	No	No	No	-
	AMES toxicity	No	No	No	Yes	-

Table 3: Phytoconstituents and drug-like properties analysis

Descriptor/Properties	Value				
	CID 10207	**CID 221493**	**CID 11349**	**CID 6604200**	**Units**
Molecular Weight	270.24	408.6	238.24	238.16	g/mol
Monoisotopic Mass	270.052826	408.287567	238.062994	238.033813	Da
Rotatable Bonds	1	4	1	3	-
H. Acceptors	5	5	3	6	-
H. Donors	3	4	1	1	-
LogP	1.3655	3.4487	3.1656	0.0735	-
Num. arom. heavy atoms	12	0	16	5	-
Fraction Csp3	0.07	0.96	0.0	0.12	-
Num. of heavy atoms	20	29	18	17	
Topological Polar Surface Area	94.83	97.99	50.44	120.73	Å²
Molar Refractivity	69.92	113.76	69.94	62.8	-

Bioavailability Radar

A molecule's radar plot needs to fall inside the colored zone to be considered drug-like (Figure 3). For each variable, the pink zone indicates the proper range, such as lipophilicity: XLOGP3 range between -0.7 to 5.0, molecular weight (Mw) ranges between 150 and 500 g/mol, topological polar surface area (TPSA) ranges between 20 and 130 Å², solubility: logS less than 6, saturation (INSATU): fraction csp3 hybridization fraction greater than 0.25, and flexibility: less than 9 rotatable bonds (Table 3). Therefore, based on the bioavailability radar indicated in Figure 3, cholic acid has oral bioavailability, while aloe-emodin and flavonol appear to be more unsaturated with respect to carbon percentage in sp3 hybridization.

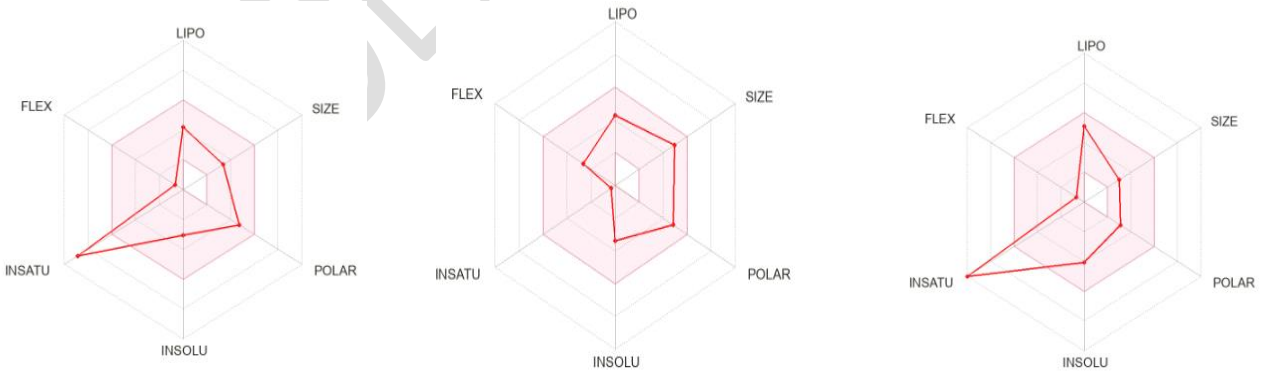

(a) (b) (c)

Figure 3: Bioavailability radar of (a) aloe-emodin, (b) cholic acid and (c) Flavonol

To conduct visual analysis, the positions for every ligand-target interaction were compared. To facilitate ligand interactions, the protein active sites were created. Initially, the analysis of the aloe-emodin-target, in which its 2D projection interaction is displayed in Figure 4(a), was deliberated. The three OH groups in aloe-emodin form hydrogen bonds with protein residues Asp47, Asp54, Asp140, Gnl133, and Phe1. In this case, aloe-emodin acts as a hydrogen donor to the polar residues Asn54 and Asp140, whereas it acts as an acceptor to the amino acid residues Asp47, Gln133, and Phe1. The bond formed here is somewhat complicated, where aloe-emodin acts as a hydrogen donor and acceptor simultaneously

The second pose is the cholic acid-target interaction, as displayed in Figure 4(b). The figure shows that cholic acid forms two OH groups in the form of hydrogen bonds with Asp140, and two oxygen bonds with Asp47 and Phe1. In this case, the Asp140 polar residue acts as a hydrogen acceptor, while the amino acid residues Asp47 and Phe1 act as donors to cholic acid oxygen atoms. It is estimated that the docking score of cholic acid is more negative than that of aloe-emodin owing to the interaction of two hydrogen bonds with the Asp140 polar residue.

The third pose is the flavonol-target interaction, as displayed in Figure 4(c). The figure illustrates that flavonol forms one OH group in the form of a hydrogen bond with Asp140 and one oxygen bond with Asn138. In this case, the Asp140 polar residue acts as a hydrogen bond acceptor, whereas Asn138 acts as a donor to a flavonol oxygen atom. In this situation, the docking score of flavonols seems to be more negative than that of aloe-emodin.

The fourth pose is the nitrofurantoin-target interaction, as displayed in Figure 4(d). This figure indicates that nitrofurantoin forms a hydrogen bond with Asp54 and an oxygen bond with Asp47, Asn135, Gnl133, and Tyr48. In this case, the Asp54 polar residue acts as a hydrogen acceptor, while Asp47, Asn135, Gnl133, and Tyr48 act as donors to a nitrofurantoin oxygen atom. In this phenomenon, the docking score of nitrofurantoin appears to be less negative than flavonol compounds.

In general, the complexity of protein-ligand interactions determines the strength of molecular docking (Madeddu et al., 2022). Aloe-emodin has hydrogen bonds with Asp47, Asp54, Asp140, Gnl133, and Phe1which are more complicated than those of cholic acid, which has two hydrogen bonds with Asp140, flavonol, and nitrofurantoin, which have a single hydrogen bond with Asp140 and Asp54, respectively. Therefore, from the visual analysis, the best compound to form a ligand target was cholic acid, followed by flavonol, aloe-emodin, and nitrofurantoin, which were endorsed by the protein-ligand interaction docking scores (Table 1).

Nitrofurantoin has become the first-line drug choice for the treatment of uncomplicated UTIs in light of updated guidelines, and its use has skyrocketed since then (Mahdizade et al, 2023). From the docking results, nitrofurantoin has a more positive value of the docking score compared with the other three ligands although both have good hydrogen bond interactions. Having the more negative value of the docking scores of aloe-emodin, cholic acid, and flavonol suggests that they might be a suitable candidate for the treatment of UTIs in comparison with the control drug.

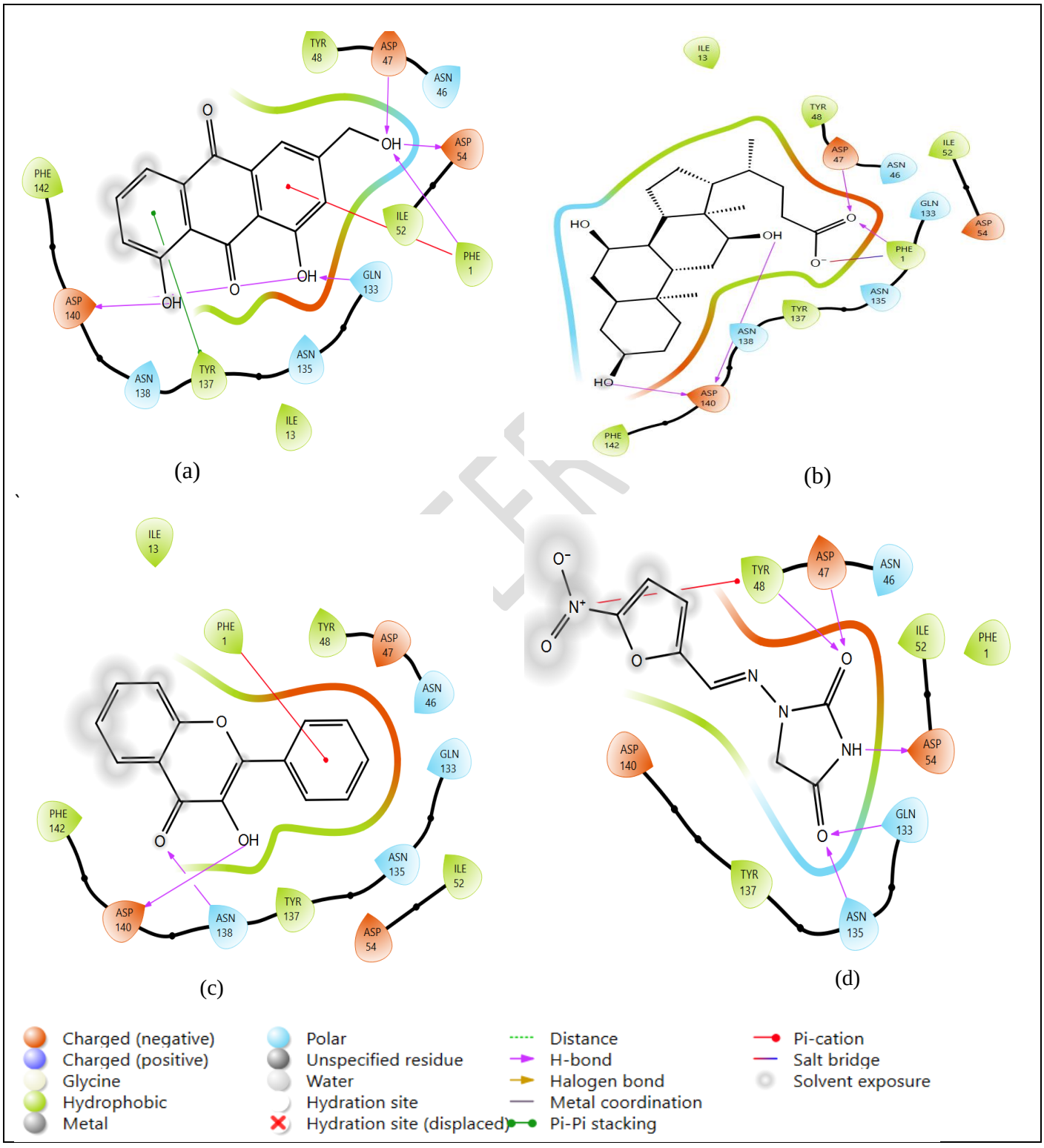
(a)
(b)
(c)
(d)
Charged (negative)
Charged (positive)
Glycine
Hydrophobic
Metal
Polar
Unspecified residue
Water
Hydration site
Hydration site (displaced)
Distance
H-bond
Halogen bond
Metal coordination
Pi-Pi stacking
Pi-cation
Salt bridge
Solvent exposure

Figure 4. Two-dimension interaction diagrams in various possess within the binding pocket 8BVD for (a) aloe-emodin, (b) cholic acid, (c) flavonol and (d) nitrofurantoin

Molecular Dynamics

Molecular dynamics is a computer modeling technique that forecasts the motion of each atom in a protein or other molecular system over time (Karplus & Mc Cammon 2002). It provides an overview of the system dynamics evolution.
Molecular dynamics (MD) was performed to examine the actual motion of atoms, which aids in understanding the detailed interaction of 8BVD with potential phytochemicals, especially when it binds to a protein target (Hansson et al, 2002). Several non-identified biological activities and intricate dynamic processes can be discovered by observing the internal dynamics of proteins (Anwer et al., 2015).

Hydrogen Bonding (H-Bonds) Analysis

The stability of a protein's three-dimensional structure is mostly determined by intramolecular hydrogen bonding within the protein molecule (Hubbard et al., 2001). Hydrogen bond analysis can also be used to examine the strength of the protein-ligand complex to assess the molecular recognition, directionality, and specificity of contacts (Mohammad et al., 2020). The analysis showed that aloe-emodin formed a maximum of 6-H bonds during the molecular dynamics computation. It was observed that aloe-emodin binds to the active pocket of 8BVD with many H-bond breakages from five to six H- bonds. From 0 to 4 ns, 1 to 5 hydrogen bonds were formed with bond breaking. From 5 to 13 ns, there were one to two stable H-bonds with fluctuations, followed by bond breaking from 13 to 18 ns. Again, from 18 to 20 ns, stable hydrogen bonds were formed, with some fluctuations (Figure 5 a).

Cholic acid formed a maximum of six H-bonds during the molecular dynamic computation. From 8 to 16 ns, a 1–2 H-bond was formed by bond breaking. From 0 to 20 ns, cholic acid bound to the active pocket of 8BVD and formed two to four H-bonds, which were the most stable, although there were some fluctuations. Stable H-bonds were formed between 4 and 5.

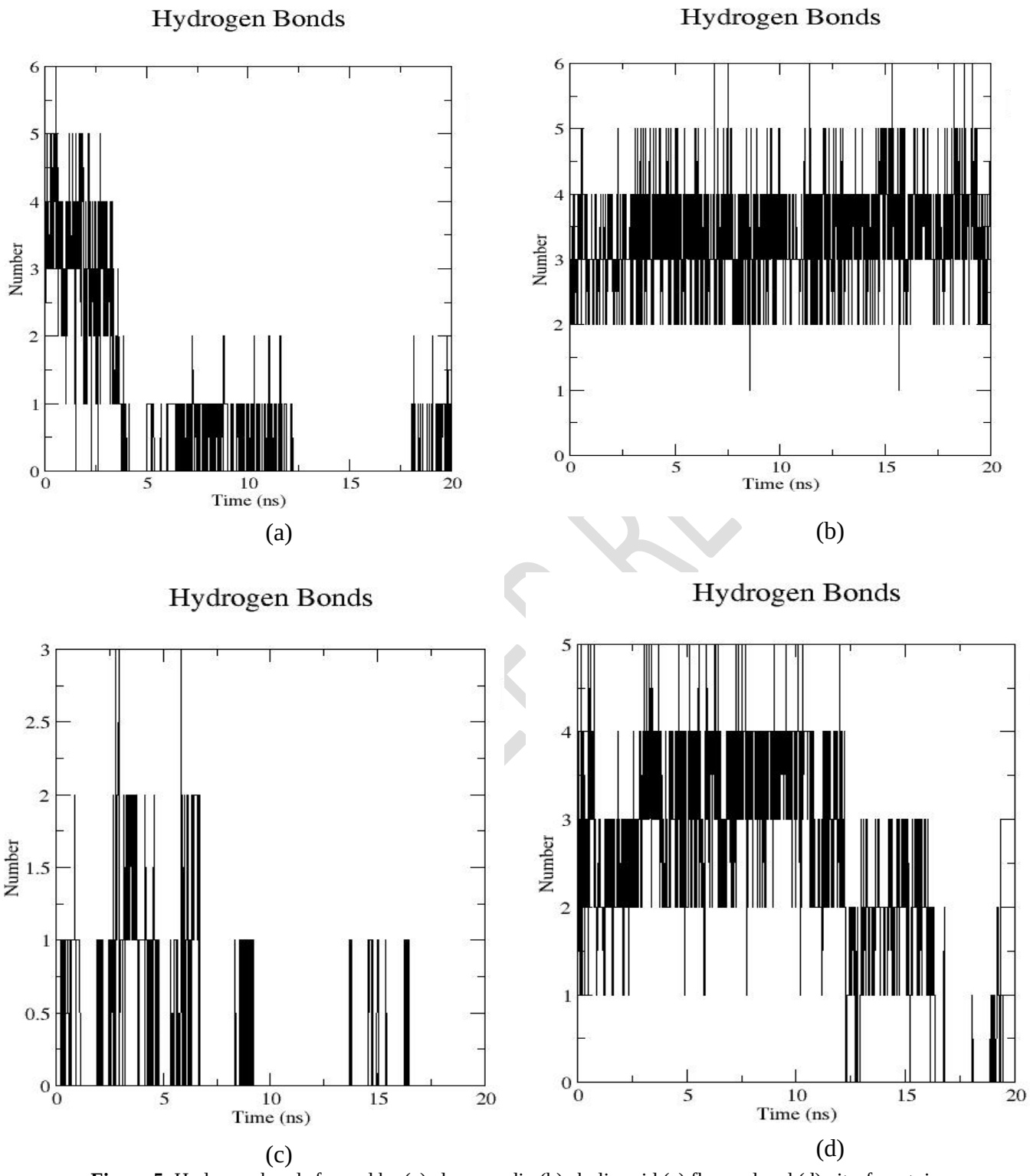

Figure 5. Hydrogen bonds formed by (a) aloe-emodin (b) cholic acid (c) flavonol and (d) nitrofurantoin

Hydrogen bonds with high fluctuations compared to the H-bonds formed between 2 two four H-bonds. Equally, from 5 to 6, hydrogen bonds were formed with bond breaking (Figure 5 b).

Molecular dynamics analysis revealed that flavonol binds to the active pocket of 8BVD and forms a 3 H-bonds. From 0 to 1ns, 0.5 to 2 H-bonds were formed, with some bond breakage. Equally, 0.5 to 3 H-bonds were formed with fluctuations and bond breakage from 2 to 7 ns. From 9 to 16 ns there a 0.5 to 1 hydrogen bond was formed with bond breakage (Figure 5 c).

Nitrofurantoin was observed to form a maximum of five H-bonds during the molecular dynamic simulation. From 12 to 20 ns, nitrofurantoin formed a 1H-bond with fluctuations and bond breakage. Similarly, 1 to 2 H-bonds were formed with some fluctuations and bond breakage, especially from 2 to 12 ns and 16 to 20 ns. Nitrofurantoin formed stable hydrogen bonds from two to four H-bonds with fluctuations and bond breakage, especially from 12 to 20 ns. Other hydrogen bonds were formed between four and five H-bonds with high fluctuations and bond breakage, particularly from 12 to 20 ns (Figure 5 d). Primarily, all four ligands had good H-bonding with the active pocket 8BVD; however, cholic acid had the most stable H-bonding in comparison to other ligands. Protein-ligand binding is highly influenced by H-bonding (Wade RC & Goodford 1989). Therefore, cholic acid has excellent potential for use as a drug candidate.

Root Mean Square Deviation (RMSD)

The root mean square deviation of each trajectory record for 20 ns in the MD simulation with regard to the initial position of the protein ligand was measured to assess the stability of the docked complex (Anusuya et al., 2015). The mean RMSD for aloe-emodin was 2.32 nm. The plot showed that aloe-emodin binds effectively more stable with 8BVD at 0.99 nm from 0 to 12 ns, and then destabilized at 13 ns to 18 ns.

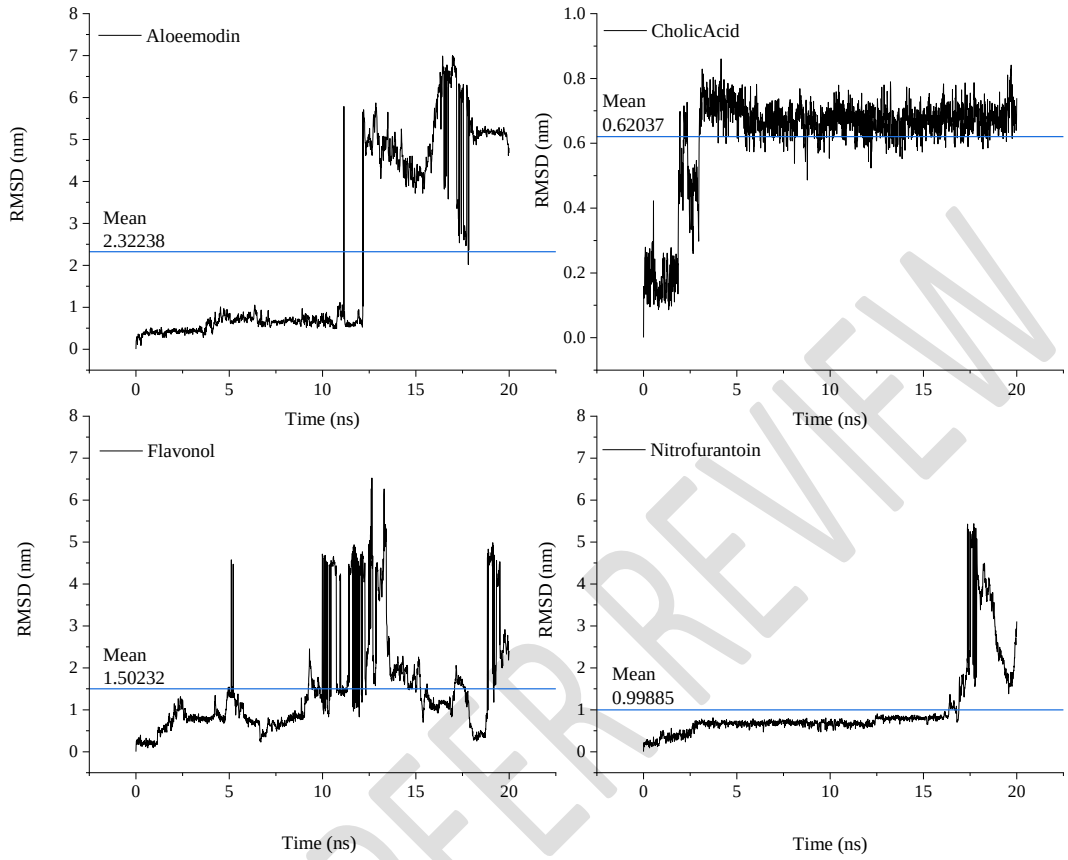

Figure 6. RMSD for aloe-emodin, cholic acid, flavonol and nitrofurantoin ligands

From the trajectory analysis, cholic acid appeared to bind more strongly with the target molecule at 0.8 nm. Initially, the ligand had a slight destabilization from 0–3 ns before stabilizing at 0.35 ns. The mean root mean square deviation (RMSD) was 0.620 nm.

The flavonol ligand was stable from 0–4 ns, before fluctuating at 5 ns. From 5.5 to 9.5 ns the ligand was re-stabilized, but then destabilized from 10 to 13 ns before gaining stability at 18 ns. The mean RMSD value was recorded at 1.50 nm.

RMSD for nitrofurantoin ligands was stable at 0.89 nm from 0 to 17 ns, and then destabilized from 18 ns up to 20 ns. The mean RMSD was recorded at 0.99 nm. Looking at their ranges, cholic acid had the lowest range followed nitrofurantoin, flavonol and aloe-emodin (Figure 6).

Root Mean Square Fluctuation (RMSF)

The flexibility of each amino acid residue, or how much it shifts or fluctuates throughout a simulation, was measured by root mean square fluctuation (RMSF), which averages the number of atoms to determine how far an atom or group of atoms has deviated from the reference structure. According to Fatriansyah et al. (2022), stable structures have lower RMSF values. The fluctuation of different atoms was observed for 20 ns, to predict the stable structure, and the RMSF was computed using the GROMACS standard function. The analysis shows that the H10 atom of aloe-emodin fluctuated more than the other atoms. The RMSF value of the H10 atom was 0.151 nm, followed by HC5 and HC6, both with RMSF value of 1.121 nm. O5, H8, and H9 atoms fluctuated at an RMSF value of 0.102 nm while the HO atoms fluctuated at 0.7 nm. The other atoms were stable at an average RMSD value of 0.03 nm (Figure 7 a).

The HC31 atom of cholic acid was perceived to have the highest fluctuation at an RMSF value of 0.186 nm, followed by HC32 and HC30 with RMSF values of 0.183 and 0.182 nm, respectively. O5, C22, and HC23 exhibited RMSF values of 0.14, 0.13 and 0.13 nm respectively. The other atoms are stable at an average RMSF value of 0.065 nm (Figure 7 b).

For the case of flavonol, the HC7 atom seems to have a higher fluctuation at an RMSF value of 0,225 nm followed by HC8 fluctuating at 0.221 nm. Both HC4 and HC5 fluctuated at the RMSF value of 0.212 nm while C14 fluctuated at 0.151nm. C10 fluctuated at the RMSF value 0f 0.150 nm followed by C9 and C13 both fluctuated at 0.149 nm. Other atoms are stable at an average RMSF value of 0.499 nm. (Figure 7 c)

In the case of nitrofurantoin, the HC7 atom had a higher fluctuation with an RMSF value of 0.209 nm, followed by HC8, HC4, and HC5 atoms with RMSF values of 0.207, 0.205, and 0.204 nm, respectively. In contrast, atoms such as C14, C13, C9, C10, and H10 also fluctuated, with RMSF values of 0.125, 0.123, 0.122, 0.123, and 0.121 nm, respectively. The other atoms appear to be stable at an average RMSF value of 0.320 nm (Figure 7 d). Most of the atoms observed to have higher RMSF values were terminal atoms.

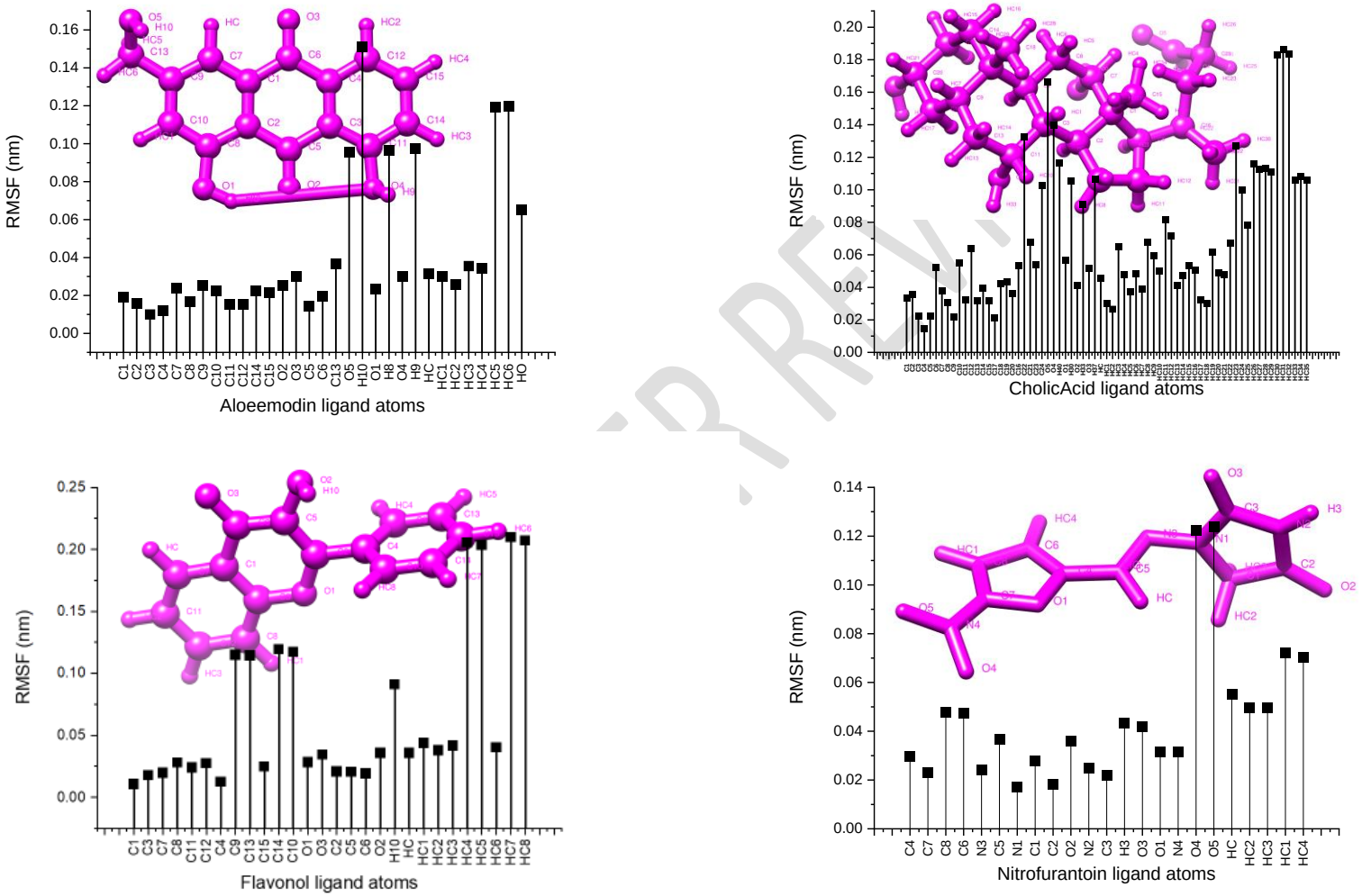

Figure 7. RMSF for aloe-emodin, cholic acid, flavonol and nitrofurantoin ligands

Radius of gyration (Rg)

The compactness of a protein structure is determined by its radius of gyration. In the protein-ligand complex, the radius of gyration of a ligand shows the ligand center of gyration to the center of gyration of the protein; therefore, a higher value of the radius of gyration indicates less stability of the structure (Lobanov et al., 2008). From the analysis, it was observed that cholic acid gyrated more, with a higher value of 0.435 nm. This higher value is attributed to the higher molecular weight of cholic acid which is 408.6 g/mol and the complex shape of the ligand (Alfred & Choi 2013).

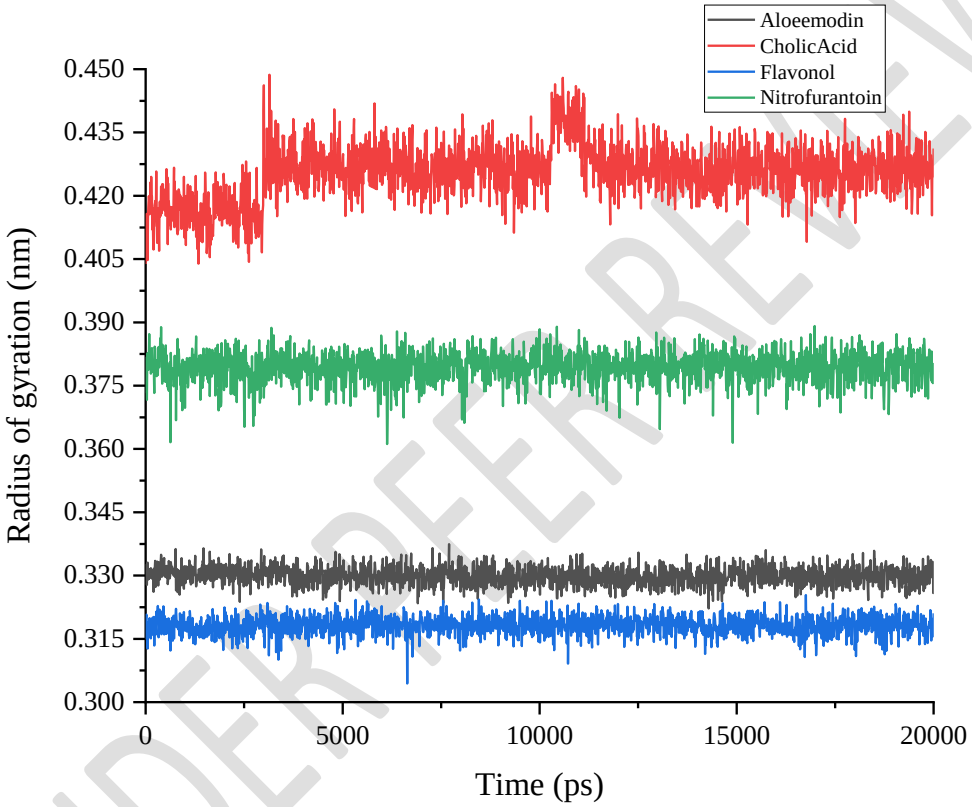

Figure 8. Radius of gyration for aloe-emodin, cholic acid, flavonol and nitrofurantoin ligands

Flavonol had the lowest Rg value of about 0.315 nm at 20 ns. The ligand gyrated with this lower value because of the simple structure of flavonol and its lower molecular weight compared to cholic acid. Other ligands such as aloe-emodin and nitrofurantoin have a minimum value of Rg ranging from 0.330 to 0.380 nm respectively at 20 ns (Figure 8).

Total Energies of the System

The quality and stability of the molecular dynamic simulations were also evaluated through a qualitative investigation of the thermodynamic properties, such as the total energies and temperature (Anwer et al., 2015). The temperature fluctuation of the trajectory was almost

constant at 300 K, indicating the stable and precise nature of the molecular dynamics simulation. The total energies of the system of both proteins and ligands were plotted as a function of MD simulation time, and the plots are shown in Figure 9.

The results from the plot illustrate that cholic acid is more stable than the other three ligands, with a total energy of -252000 kJ/mol. Aloe-emodin, flavonol, and nitrofurantoin ligands were also stable, with slightly higher energies ranging from -248000 to -246000 KJ/mol. The trajectory profile's lower energy suggests that the system was remarkably stable during the simulation (Lakshmi et al., 2020).

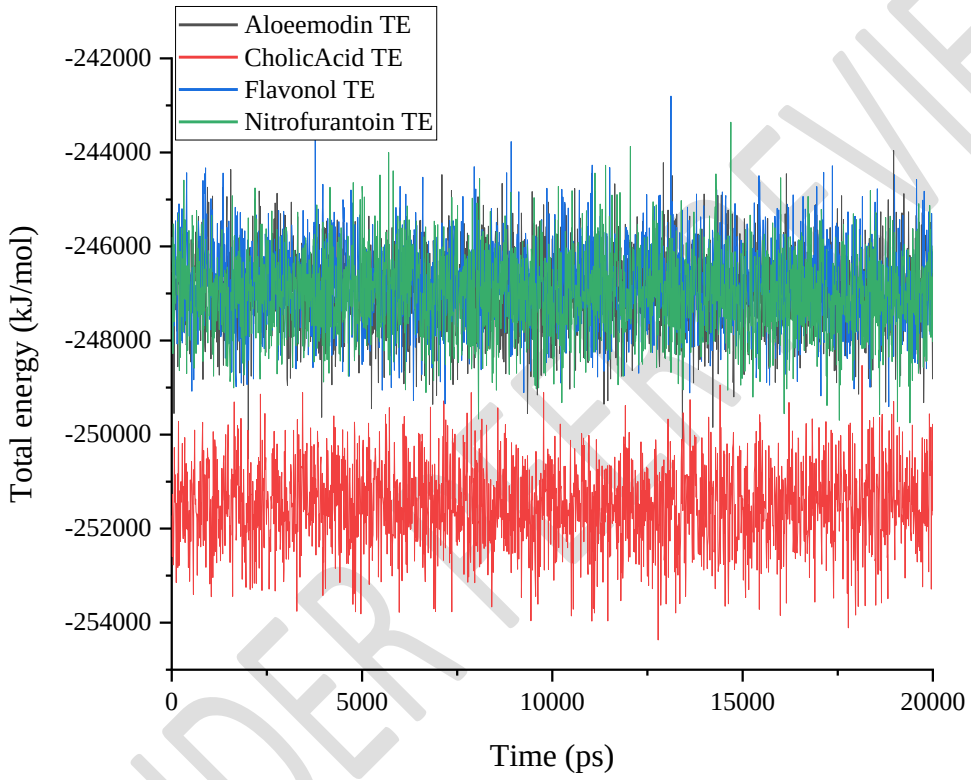

Figure 9. Total Energies of the System during the MD simulation

Conclusion

UPEC inhibition is an innovative approach for preventing the emergence of UTIs. Natural compounds are the most important source of medicines for the treatment of many diseases (Veeresham 2012). The ligand-target complex presented a good candidate for molecular docking and molecular dynamics. All ligands were superb candidates as 8BVD inhibitors based on the molecular docking scores, ADMET studies, and drug-like characteristics. Docking score ranges were arranged as follows from high to low as follows: cholic acid, flavonol, aloe-emodin, and nitrofurantoin. These results suggest that cholic acid is a more suitable inhibitor than other ligands. Molecular dynamics revealed that all ligands can also serve as excellent inhibitors, although

fluctuations in aloe-emodin and flavonol remain high. However, additional studies and tests are required to validate these compounds as 8BVD protein inhibitors.

Reference

Abe, C.M.; Salvador, A.; Falsetti, I.N.; Blanco, E.; Blanco, M. (2008). Uropathogenic Escherichia coli (UPEC) strains may carry virulence properties of diarrhoeagenic E. coli. FEMS Immunol. *Med. Microbiol.*, *52*, pg 397–406. DOI: 10.1111/j.1574-695X.2008.00388.x

Alfred Rudin, Phillip Choi. (2013). the Elements of Polymer Science & Engineering (Third Edition), Science Direct, Elsevier Inc.

Anwer, K., Sonani, R., Madamwar, D., Singh, P., Khan, F., Bisetty, K., Ahmad, F., & Hassan, M. I. (2015). Role of N-terminal residues on folding and stability of C-phycoerythrin: simulation and urea-induced denaturation studies, *Journal of Biomol Structure Dynamics*, *33*(1), pg 121-133. https://doi.org/10.1080/07391102.2013.855144

Anusuya, S., Velmurugan, D., Gromiha, M.M., (2015). Identification of dengue viral RNA-dependent RNA polymerase inhibitor using computational fragment based approaches and molecular dynamics study. *J. Biomol. Struct. Dyn*. 34 (7), pg 1512–1532. https://doi.org/10.1080/07391102.2015.1081620

Asadi Karam, M. R., Habibi, M., & Bouzari, S. (2019). Urinary tract infection: Pathogenicity, antibiotic resistance and development of effective vaccines against Uropathogenic Escherichia coli. *Mol Immunol*, 108, pg 56-67. https://doi.org/10.1016/j.molimm.2019.02.007

Beda John Mwang'onde, Josefine Innocent Mchami.(2022).The aetiology and prevalence of urinary tract infections in Sub-Saharan Africa: a Systematic Review, *J. Health Biol Sci*.;10(1):pg 1-7

Burak M & Imen Y .(1999). Flavonoids and their antioxidant properties. *Turkiye Klin Tip Bil Derg* vol 19, pg 296–304.

Chhaya Shah, Ratna Baral, Bijay Bartaula and Lok Bahadur Shrestha. (2019). Virulence factors of uropathogenic Escherichia coli (UPEC) and correlation with antimicrobial resistance, *BMC Microbiology Journal*, 19 (204). https://doi.org/10.1186/s12866-019-1587-3

Christopher A Lipinski; Franco Lombardo; Beryl W Dominy; Paul J Feeney. (2001). Experimental and computational approaches to estimate solubility and permeability in drug discovery and development settings, *Advanced Drug Delivery Reviews 46(1-3), pg 3–26.* doi:10.1016/s0169-409x(00)00129-0

Daina, A., Michielin, O. & Zoete, V. (2017).SwissADME: a free web tool to evaluate pharmacokinetics, drug-likeness and medicinal chemistry friendliness of small molecules. *Sci Rep* 7, (42717) https://doi.org/10.1038/srep42717

David Camp, Agatha Garavelas, and Marc Campitelli. (2015). Analysis of physicochemical properties for drugs of natural origin, *J. Nat. Prod*. 78, (6), pg 1370–1382. DOI: 10.1021/acs.jnatprod.5b00255

Dong X, Zeng Y, Liu Y, You L, Yin X, Fu J, Ni J. (2020). Aloe-emodin: A review of its pharmacology, toxicity, and pharmacokinetics. *Phytother Res*. 34(2) pg 270-281. doi: 10.1002/ptr.6532.

Douglas E. V. Pires, Tom L. Blundell, and David B. Ascher .(2015). pkCSM: Predicting small-molecule pharmacokinetic and toxicity properties using graph-based signatures, *Journal of medicinal chemistry*, (58) pg 4066−4072. https://doi.org/10.1021/acs.jmedchem.5b00104

Flores-Mireles, A.L.; Walker, J.N.; Caparon, M.; Hultgren, S.J.(2015).Urinary tract infections: Epidemiology, mechanisms of infection and treatment options. *Nat. Rev. Microbiol*,13, pg 269–284. DOI: 10.1038/nrmicro3432

Gerard J. Kleywegt and T. Alwyn Jones. (1997).Model building and refinement practice. *In Methods in enzymology* (Volume 277, 1997, Pages 208-230). https://doi.org/10.1016/S0076-6879(97)77013-7

Gurisha, M.S., Rao, P.V.K. and Cherupally, L. (2024) Phytochemicals of Aloe barbadensis miller as Potential Inhibitors of Uropathogenic Escherichia coli for Urinary Tract Infection Therapy: An in Silico Approach. Open Jour nal of Biophysics, 14, 99-120. https://doi.org/10.4236/ojbiphy.2024.142006

Haidan Yuan, Qianqian Ma, Li Ye and Guangchun Piao.(2016) The traditional medicine and modern medicine from natural products, review, *MDPI Journal of Molecules*, Vol 21, pg 559. DOI: 10.3390/molecules21050559

Hansson, T., C. Oostenbrink, and W. F. van Gunsteren. (2002). Molecular dynamics simulations. *Curr. Opin. Struct. Biol.* vol 12 pg 190–196.

Honório KM, Moda TL, Andricopulo AD. Pharmacokinetic properties and in silico ADME modeling in drug discovery. Med Chem. 2013 Mar;9(2):163-76. doi: 10.2174/1573406411309020002.

Huang, C.C., Couch, G.S., Pettersen, E.F., and Ferrin, T.E. (1996)."Chimera: an extensible molecular modeling application constructed using standard components." *Pacific Symposium on Biocomputing* 1:724

Hubbard, R.E.; Kamran Haider, M. (2001). Hydrogen bonds in proteins: role and strength. *In eLS; John Wiley & Sons*, Ltd.: Hoboken, NJ, USA.

Hu Q, Feng M, Lai L, Pei J. (2018). Prediction of Drug-Likeness Using Deep Autoencoder Neural Networks. *Front Genet*. 27 (9) 585. doi: 10.3389/fgene.2018.00585.

Fatriansyah JF, Rizqillah RK, Yandi MY, Fadilah, Sahlan M. (2022). Molecular docking and dynamics studies on propolis sulabiroin-A as a potential inhibitor of SARS-CoV-2. J King Saud Univ Sci. Jan;34(1):101707. doi: 10.1016/j.jksus.2021.101707.

Jia C-Yang, Li J-Yi, Hao G-Fei, Yang G-Fu .(2019). A drug-likeness toolbox facilitates ADMET study in drug discovery, *Drug Discovery Today* https://doi.org/10.1016/j.drudis.2019.10.014

J. P. Walters, C. M. Rogers, and S. P. Crago .(2014). Maestro software and application performance, *Conference Paper*, GOMACTech-14 conference.

Karplus M, and McCammon JA (2002). Molecular dynamics simulations of biomolecules. *Nature structural biology* 9, 646–652.

Kim, S., Chen, J., Cheng, T., Gindulyte, A., He, J., He, S., Li, Q., Shoemaker, B. A., Thiessen, P. A., Yu, B., Zaslavsky, L., Zhang, J., & Bolton, E. E. (2023). *PubChem 2023 update. Nucleic Acids Res*., 51(D1), D1373–D1380.https://doi.org/10.1093/nar/gkac956

Lobanov, M.Y., Bogatyreva, N.S. & Galzitskaya, O.V. (2008). Radius of gyration as an indicator of protein structure compactness. *Mol Biol* 42, pg 623–628 https://doi.org/10.1134/S0026893308040195

Maan, A. A., Nazir, A., Khan, M. K. I., Ahmad, T., Zia, R., Murid, M., & Abrar, M. (2018). The therapeutic properties and applications of Aloe vera : A review. *Journal of Herbal Medicine, 12, 1–10.* doi:10.1016/j.hermed.2018.01.002

Madeddu, F.; Di Martino, J.; Pieroni, M.; Del Buono, D.; Bottoni, P.; Botta, L.; Castrignanò, T.; Saladino, R. (2022). Molecular docking and dynamics simulation revealed the potential

inhibitory activity of new drugs against human topoisomerase I receptor. *Int. J. Mol. Sci. 23*, 14652. https://doi.org/10.3390/ ijms23231465

Mahdizade Ari M, Dashtbin S, Ghasemi F, Shahroodian S, kiani P, Bafandeh E, Darbandi T, Ghanavati R and Darbandi A (2023) Nitrofurantoin: properties and potential in treatment of urinary tract infection: a narrative review. Front. Cell. Infect. Microbiol. 13:1148603. doi: 10.3389/fcimb.2023.1148603

Mehdi Goudarzi, Saeedeh Ghafari, Masoumeh Navidinia and Hadi Azimi. (2018). Aloe vera gel: effective therapeutic agent against extended-spectrum β-lactamase producing escherichia coli isolated from patients with urinary tract infection in Tehran-Iran, *Journal of Pure and Applied Microbiology*, Vol. 11(3), pg 1401-1408. https://dx.doi.org/10.22207/JPAM.11.3.22

Mousavifar, L. Sarshar, M. Bridot, C. Scribano, D.Ambrosi, C. Palamara, A.T. Vergoten, G. Roubinet, B. Landemarre, L, Bouckaert, J. et al. (2023).Insightful Improvement in the Design of Potent Uropathogenic E. coli FimH Antagonists. *Pharmaceutics* 15,(2) pg 527. doi: 10.3390/pharmaceutics15020527

Panche AN, Diwan AD, Chandra SR. (2016). Flavonoids: an overview. *J Nutr Sci*. vol 5:pg 47. doi: 10.1017/jns.2016.41.

Pettersen, E.F., Goddard, T.D., Huang, C.C., Couch, G.S., Greenblatt, D.M., Meng, E.C., and Ferrin, T.E. (2004)."UCSF Chimera A Visualization System for Exploratory Research and Analysis." *J. Comput. Chem. 25*(13): pg 1605-1612. https://doi.org/10.1002/jcc.20084

Preman Geetika, Muskaan Mulani, Ayesha Bare, Khushboo Relan, Leebah Sayyed, Vikas Jha, Kavita Pandey. (2022). Screening of phytochemicals for anti-Tubercular potential using molecular docking approach. *J Tuberc*.; 5(1): pg 1030.

Rao P, Shukla A, Parmar P, Rawal RM, Patel B, Saraf M, Goswami D. (2020). Reckoning a fungal metabolite, pyranonigrin A as a potential main protease (Mpro) inhibitor of novel SARS-CoV-2 virus identified using docking and molecular dynamics simulation. *Biophys Chem*. Vol 264 pg 106425. doi: 10.1016/j.bpc.2020.106425.

Salaria D, Rajan R, Mehta J, Awofisayo O,Olatomide A. Fadare,OA, Balvir K, Renato AC, Shikha RC, Neha K, Eun HC, Nagendra KK. (2022). Phytoconstituents of traditional Himalayan Herbs as potential inhibitors of Human Papillomavirus (HPV-18) for cervical cancer treatment: An In silico Approach. *PLoS ONE* 17(3): pg 1-20. https://doi.org/10.1371/journal.pone.0265420

Seifu WD, Gebissa AD. (2018). Prevalence and antibiotic susceptibility of uropathogens from cases of urinary tract infections (UTI) in shashemene referral hospital, Ethiopia. *BMC Infect Dis*.18(1) pg 30. doi: 10.1186/s12879-017-2911-x.

Selvaraj A. Lakshmi, Raja M. B. Shafreen, Arumugam Priya & Karutha P. Shunmugiah. (2021). Ethnomedicines of Indian origin for combating COVID-19 infection by hampering the viral replication: using structure-based drug discovery approach, *J. of Biomolecular Structure and Dynamics*, 39(13), pg 4594-4609, DOI: 10.1080/07391102.2020.1778537

S.B. Udugade, R.C Doijad, B. V. Udugade. (2019). In silico evaluation of pharmacokinetics, drug-likeness and medicinal chemistry friendliness of momordicin1: an active chemical constituent of momordica charantia, J Adv Sci Res, 10 (3) gp 222-229.

Stanzione, F., Giangreco, I., & Cole, J. C. (2021). Use of molecular docking computational tools in drug discovery. *Progress in Medicinal Chemistry, 273–343.* doi:10.1016/bs.pmch.2021.01.004

Taj M, Shiza S, Anas S , Mohamed F. Alajmi, Afzal H, Asimul I, Faizan A and Imtaiyaz H.(2020). Virtual screening approach to identify high-affinity inhibitors of serum and glucocorticoid-regulated kinase 1 among bioactive natural products: combined molecular docking and simulation studies, *MDPI Journal of molecules*. 13;25(4):823. doi: 10.3390/molecules25040823.

Terlizzi ME, Gribaudo G, Maffei ME. (2017). UroPathogenic *Escherichia coli* (UPEC) Infections: Virulence Factors, Bladder Responses, Antibiotic, and Non-antibiotic Antimicrobial Strategies. *Front Microbiol.* (8):1566. doi: 10.3389/fmicb.2017.01566.

Tomas Hansson; Chris Oostenbrink; WilfredF van Gunsteren (2002). Molecular dynamics simulations. current opinion in structural biology, 12(2), 190–196. doi:10.1016/s0959-440x(02)00308-1

Tripathi Kishua, Kumar T. Siva. (2010). Antibacterial activity of organometallic complexes of cholic acid, *Dige J of Nanomat and Biostr,* Vol. 5, No 3 p. 763-770.

Van Der Spoel D, Lindahl E, Hess B, Groenhof G, Mark AE, Berendsen HJ (2005). "GROMACS: fast, flexible, and free". *J Comput Chem*. 26 (16): pg 1701-1718. doi:10.1002/jcc.20291

Veeresham C. (2012). Natural products derived from plants as a source of drugs. *J Adv Pharm Technol Res*. 3(4): pg 200. doi: 10.4103/2231-4040.104709. PMID: 23378939; PMCID: PMC3560124.

Wade RC, Goodford PJ. (1989). The role of hydrogen-bonds in drug binding. *Prog Clin Biol Res*.;289: pg 433-44. PMID: 2726808.

Wu, J.; Yu, T.T.; Kuppusamy, R.; Hassan, M.M.; Alghalayini, A.; Cranfield, C.G.; Willcox, M.D.P.; Black, D.S.; Kumar, N. (2022). Cholic acid-based antimicrobial peptide mimics as antibacterial agents. *Int. J. Mol. Sci.* vol 23, pg 4623. https:// doi.org/10.3390/ijms23094623

Zagaglia, C.; Ammendolia, M.G.; Maurizi, L.; Nicoletti, M.; Longhi, C. (2022). Urinary tract infections caused by uropathogenic escherichia coli strains—*New Strategies for an old pathogen. microorganisms* 10, pg 1425. https://doi.org/10.3390/ microorganisms10071425.